Novel *PTH* gene mutations causing isolated hypoparathyroidism

[1,2,3]Colin P. Hawkes, MD, PhD, [4]Jamal M. Al Jubeh, MD [5]Dong Li, PhD [6,7]Susan E. Tucker, MD [6]Tara Rajiyah, MD and [1,2]Michael A. Levine, MD

[1]Division of Endocrinology and Diabetes, The Children's Hospital of Philadelphia, Philadelphia, PA, 19104 USA.

[2]Perelman School of Medicine, University of Pennsylvania, Philadelphia, PA, 19104 USA.

[3]Department of Paediatrics and Child Health, University College Cork, Cork, Ireland.

[4]Department of Pediatrics, Sheikh Khalifa Medical City, Abu Dhabi, United Arab Emirates.

[5]Center for Applied Genomics, The Children's Hospital of Philadelphia, Philadelphia, PA, 19104 USA

[6]Section of Adult and Pediatric Endocrinology, Diabetes, and Metabolism, The University of Chicago, Chicago, IL 60611 USA

[7]Current CHG Healthcare, Midville, UT 84047

Disclosure Summary: CPH, JMAJ, DL, SET, TR, and MAL have nothing to declare.

Correspondence should be addressed to

Dr. Michael A. Levine, Division of Pediatric Endocrinology and Diabetes, The Children's Hospital of Philadelphia, ARC510A, 3615 Civic Center Blvd, Philadelphia, PA, 19104.

Email: levinem@chop.edu

Tel: 01-215-590-3618

Fax: 01-215-590-3053

ORCID ID

Colin P. Hawkes: 0000-0001-6484-0445

Michael A. Levine: 0000-0003-0036-7809

Abstract

Abbreviations

cAMP = cyclic adenine monophosphate

CASR = calcium-sensing receptor

SQ = Subcutaneous

GCM2 = glial cells missing-2

GNA11 = G protein α11

PTH = parathyroid hormone

Funding Sources: Children's Hospital of Philadelphia Research Institute and the National Institutes of Health (R01 DK112955 to MAL).

Acknowledgements: The authors gratefully acknowledge the family members who participated in these studies as well as the excellent technical assistance of Mr. Harsh Kanwar. We also thank Dr. Thomas Gardella, Massachusetts General Hospital, for thoughtful discussion of our work. This work was supported in part by the Children's Hospital of Philadelphia Research Institute and the National Institutes of Health (R01 DK112955 to MAL).

Abstract

Context: *PTH* gene mutations represent a rare cause of familial isolated hypoparathyroidism (FIH). These defects can cause hypoparathyroidism with increased or decreased serum levels of PTH through 1) impaired PTH synthesis; 2) induction of parathyroid cell apoptosis; or 3) secretion of bioinactive PTH molecules. Eight pathogenic mutations of this gene have been described previously.

Objective: Through describing two novel mutations of the *PTH* gene, we aim to extend the molecular basis for FIH and further refine the proposed mechanisms by which *PTH* mutations cause hypoparathyroidism.

Design: Proband case reports with extended family analysis.

Patients and Other Participants: The probands in both kindreds presented before 10-days-of-age with hypocalcemia and elevated phosphate levels. Proband A had low PTH levels, while these levels were elevated in Proband B. Proband B was initially diagnosed with pseudohypoparathyroidism.

Interventions: Methylation analysis of CpG dinucleotides within three *GNAS* differentially methylated regions; Whole genome sequencing; and PTH infusion with analysis of nephrogenous cyclic AMP.

Results: Proband A had a novel heterozygous sequence change in exon 2 of the *PTH* gene, c.46_47delinsAA (p.Ala16Lys) and Proband B had a novel homozygous nucleotide transition in *PTH* exon 3 (c.128G>A; p.G43E) that led to replacement of glycine by glutamic acid at position 12 of PTH 1-84. PTH 1-34 infusion demonstrated that renal responsiveness to PTH was intact and not antagonized by circulating bioinactive PTH.

Conclusions: *PTH* gene mutations are uncommon causes of hypoparathyroidism, but can be misdiagnosed as disorders of gland development or receptor function if PTH levels are

decreased or elevated, respectively. Genetic testing should be considered early in the diagnostic approach to these presentations.

Keywords: parathyroid, hypoparathyroidism, hypocalcemia, genetic, bioinactive, PTH.

Introduction

Familial isolated hypoparathyroidism (FIH) is an uncommon condition that is associated with mutations in genes that are required for structural or functional integrity of the parathyroid glands. The most common molecular pathology in FIH is related to genetic defects that lead to activation of the calcium-signaling pathway and which inhibit secretion of parathyroid hormone (PTH) from otherwise normal parathyroid glands. This condition has been termed Autosomal Dominant Hypocalcemia and is usually associated with gain-of-function mutations in the genes encoding the calcium sensing receptor (*CASR*, Autosomal dominant hypocalcemia type 1; OMIM 601198) (1) or the alpha subunit of the G11 protein (*GNA11*, Autosomal dominant hypocalcemia type 2; OMIM 615361) (2-4) that couples the CASR to intracellular signaling (5). A second and less common mechanism is the lack of development or survival of parathyroid cells, a condition that is most commonly associated with recessive loss-of-function (6-9) or dominant negative (10-12) mutations (OMIM 618883) in the *GCM2* gene, which encodes a transcription factor that has been termed the master regulator of parathyroid development (13, 14).

A third form of FIH is due to dominant or recessive mutations in the *PTH* gene (OMIM 168450) located at 11p15.3 (15) that impair secretion of bioactive PTH molecules. Although only eight mutations have been described in the *PTH* gene (16) to date, these genetic defects lead to hypoparathyroidism through at least three different pathophysiological mechanisms, including impaired synthesis of PTH (17), induction of an endoplasmic reticulum (ER) stress response that leads to apoptosis of the parathyroid cells (18-21), or secretion of bioinactive PTH molecules (22, 23). Here we describe two novel mutations in the *PTH* gene that extend the molecular basis for FIH and further refine the proposed mechanisms by which *PTH* mutations cause hypoparathyroidism.

Methods

This study was approved by the institutional review board of the Children's Hospital of Philadelphia. Written informed consent, and assent as appropriate, was obtained from all participants.

We recruited two subjects and all available family members and collected clinical and molecular data. The diagnosis of functional hypoparathyroidism was based on the presence of hypocalcemia and hyperphosphatemia; serum levels of PTH were low in the subject from family A and elevated in affected members of family B, who were initially suspected to have pseudohypoparathyroidism (PHP) type 1B (PHP1B). Not all subjects were able to undergo all analyses.

Genetic sequence analyses

Peripheral blood DNA was extracted from all subjects using standard techniques. Genomic DNA from proband of family A (Figure 1A) was subjected to targeted genetic analysis using a commercial gene panel (University of Chicago Genetic Services Laboratory Hypoparathyroidism Panel) that enabled assessment of twenty genes (*AIRE, AP2S1, CASR, CHD7, CYP24A1, FAM111A, GATA3, GCM2, GNA11, GNAS, HADHA, HADHB, PDE4D, PRKAR1A, PTH, PTH1R, SOX3, STX16, TBCE, and TBX1*) that have been linked to parathyroid disturbances using next generation sequencing.

Whole genome sequencing (WGS) was performed for members of kindred B (Figure 1B) using previously described methods (24). Briefly, all the raw reads were aligned to the reference human genome using the Burrows-Wheeler Aligner (BWA-Mem) (25) and single-nucleotide variants (SNVs) and small insertions/deletions (INDELs) were captured using the

Genome Analysis Tool Kit (GATK) (26). The kinship coefficient was calculated between every two samples via KING (27) to confirm reported relationships.

All variants were confirmed by Sanger sequencing. The potential pathogenicity of all genetic variants that we identified was assessed using Polyphen-2 (28), SIFT (29), and MutationTaster (30). The classification of the genetic variants was performed using criteria recommended by the American College of Medical Genetics and Genomics (31). We analyzed the effect of amino acid replacements on secondary structure of PTH (1-84) using Chou-Fasman, Garnier-Osguthorpe-Robson, and Neural Network methods (http://cib.cf.ocha.ac.jp/bitool/MIX/) (32-34).

We used two publicly available databases, the Single Nucleotide Polymorphism Database (https://www.ncbi.nlm.nih.gov/projects/SNP/) and the Exome Aggregation Consortium (http://exac.broadinstitute.org/), to identify previous reports of sequence variants. We used the MUSCLE (multiple sequence comparison by log-expectation) online tool (http://www.ebi.ac.uk/Tools/msa/muscle/) to evaluate phylogenetic conservation of affected codons. The potential effect of missense mutations on signal peptide function was evaluated using SignalP, version 5 (https://services.healthtech.dtu.dk/service.php?SignalP-5.0) (35).

GNAS Gene Methylation Analysis

Bisulfite treatment of genomic DNA and pyrosequencing analysis was performed on DNA from patients VI-2 and VI-3 (Figure 1B) from kindred B using the PSQ™96HS system as previously described (24, 36). We also used assay ADS1410 to analyze methylation of the DMR of the maternally imprinted gene *NNAT* encoding neuronatin on chromosome at 20q11.23 (20:g.36149607-36152092) as a control for global methylation defects. All experimental conditions are available upon request. The amount of C relative to the sum of C and T at each CpG was determined, and we calculated the average of the percentage

numbers for all sites in a particular DMR to determine the DMR methylation level (scale, 0-100).

Biochemical analyses

All biochemical analyses were performed using standard clinical assays. Serum concentrations of 25-hydroxyvitamin D (25(OH)D) and 1,25-dihydroxyvitamin D (1,25(OH)2D) were measured by LC/MS-MS (CHOP). Serum intact PTH levels were determined by commercial immunoassays; for kindred A we used an immunoassay for intact PTH performed on a Siemens IMMULITE 2000 while for kindred B we used the Roche e801 Elecsys assay in which a biotinylated monoclonal antibody reacts with epitopes in the amino acid regions 26-32 and a second antibody reacts with epitopes in amino acid region 37-42 of the mature PTH 1-84. FGF23 levels were measured by Mayo Clinic Laboratories using an immunoassay that detects c-terminal fragments and intact FGF23. Tubular maximum phosphate reabsorption per GFR (TmP/GFR) was calculated using the Walton and Bijvoet nomogram (37). Concentrations of urinary cyclic AMP were measured using the Enzo Life Sciences cAMP ELISA kit (Catalog # ADI-900-067, RRID:AB_2814712).

PTH Infusion Protocol: PTH infusion was performed using a protocol based on that previously described (38, 39). A dose of 40 μg of human recombinant PTH 1-34 (teriparatide) was administered subcutaneously at time 0. Urinary creatinine, phosphorus, calcium, and cyclic AMP were measured at -60, -30, 0, 30, 60, 90, 120, 180, and 240 minutes. Serum creatinine, phosphorus, and intact PTH were measured at 0, 30, 60, 90, 120, 180, and 240 minutes.

Statistical Analyses: Results are presented as the mean ± SD, and comparisons between groups were analyzed by one-way ANOVA with Dunnett's posttest using GraphPad InStat version 3.10 for Windows (GraphPad Software, San Diego California USA, www.graphpad.com).

Results

Case Reports

Kindred A. The proband (Figure 1A) is an African American male who was born at term following an uncomplicated pregnancy. He had been formula-fed with appropriate weight gain but at 8-days-of-age he was admitted to hospital after a prolonged generalized, tonic-clonic seizure, preceded by twitching of his upper and lower limbs on the day of presentation. Biochemical investigation demonstrated a serum calcium concentration of 1.3 mmol/L (ref 1.9-2.6), ionized calcium concentration of 0.6 mmol/L (ref 1.1-1.4), inorganic phosphate level of 4.1 mmol/L (ref 1.5-2.9), magnesium level of 0.7 mmol/L (ref 0.7-1), 25(OH)D concentration of 24.5 nmol/L (ref 75-250), and intact PTH level of 0.6 pmol/L (ref 1.1-6.9). Alkaline phosphatase and renal function were normal. Physical examination was notable for a high-pitched holosystolic murmur, hypertelorism, and an exaggerated Moro reflex that evolved into active convulsions. An echocardiogram demonstrated a small ventricular septal defect with left-to-right shunting and a very small patent foramen ovale. Genetic testing for DiGeorge sequence was negative, and a SNP microarray was normal. Intact PTH levels remained low. He has been treated with elemental calcium plus calcitriol.

Kindred B

The proband, patient VI-2 and his brother VI-3 each presented at 10-days-of-age with hypocalcemia. They are white and from the United Arab Emirates. A sister (VI-5) is also affected. Their consanguineous parents and two other siblings are unaffected, but there are many maternal and paternal aunts and uncles who are also affected (Figure 1B and Table 1). The proband, now 11 years of age, presented with a seizure at age 10 days and was found to have very low serum calcium level (1.4 mmol/L) with elevated levels of phosphorus and PTH. He also had severe vitamin D deficiency that was treated as well. His current

treatment is elemental calcium plus alfacalcidol daily. Both brothers showed normal growth and development. All affected subjects had markedly elevated serum levels of PTH, hypocalcemia, and hyperphosphatemia (Table 1). Based on these laboratory findings the proband and his affected sibs were initially diagnosed as a possible form of autosomal recessive pseudohypoparathyroidism (PHP) type 1b (40).

Methylation analysis

We used quantitative pyrosequencing to assess the methylation status of CpG dinucleotides within three *GNAS* DMRs that are associated with methylation defects in subjects with PHP1b (36) in members of family B. Our pyrosequencing analyses showed that both VI-2 and VI-3 had normal methylation at each DMR tested (Table 2).

Gene sequencing

Genomic DNA from the proband in kindred A (Figure 1A) revealed a novel heterozygous sequence change in exon 2 of the *PTH* gene, c.46_47delinsAA (p.Ala16Lys). Analysis of parental DNA samples was negative for the variant. The p.Ala16Lys variant occurs within the hydrophobic core of the leader sequence of preproparathyroid hormone (preproPTH; Figure 2). The variant is not present in either the Single Nucleotide Polymorphism Database or Exome Aggregation Consortium database, making unlikely the possibility that the variant is a rare polymorphism. A phylogenetic analysis showed that alanine-16 is highly conserved among orthologs and therefore likely to have functional significance and its replacement is therefore considered to be pathogenic. The p.A16K substitution is flanked by two other similar heterozygous missense mutations, p.M14K and p.C18R, that have been linked to hypoparathyroidism through a mechanism in which defective processing of the leader sequence leads to intracellular retention of the nascent mutant protein, predominantly in the ER, with subsequent induction of the unfolded protein response and apoptosis (18-21). Similar to Cinque et al (19), we used the SignalP hidden Markov model program (version

5.0) to analyze the amino acid sequence of the p.A16K preproPTH proteins. The program correctly identified a signal sequence within the wildtype preproPTH protein (probability, 0.954) with a cleavage site between positions +25 and +26 (SDG-KS; probability of 0.889) (Figure 3A). These analyses further predicted that the signal peptide has an n-region from amino acid 1 to 9, a hydrophobic core h-region from amino acid 10 to 20, and a c-region from amino acid 21 to 25. The SignaIP analysis of the preproPTH protein in which Ala-16 is replaced by Lys shows a markedly reduced probability (0.483) that the variant protein contains a signal peptide and fails to identify a functional cleavage site (Figure 3B). Therefore, these *in silico* analyses for p.A16K, in the context of similar *in silico* results (Figure 3C and 3D) and experimental data for p.M14K and p.C18R, suggest that defective processing of the leader sequence of these preproPTH molecules leads to ER stress-induced parathyroid cell death and provides an underlying mechanism for FIH due to these heterozygous missense mutations in the *PTH* gene.

WGS revealed a novel homozygous nucleotide transition in *PTH* exon 3 (c.128G>A) in the proband of family B, V1-2 (Figure 1) that results in substitution of glycine at codon 43 to glutamic acid (p.G43E), which corresponds to amino acid 12 in the mature 1-84 PTH molecule (Figure 2). WGS did not disclose any other genetic variants in *GNAS* that could be disease-causing (data not shown). The glycine at position 12 is highly conserved among the mature PTH proteins of all known species and is one of the few amino acids that is identical in PTH and PTHrP, consistent with its importance in the interaction of these molecules with their shared receptor, the type 1 PTH receptor (PTHR1). The structural elements of PTH and PTHrP that are required for receptor binding and biological activity are two helical segments, one N-terminal and one C-terminal, connected by hinges or flexible points located around positions 12 and 19 (41, 42). The biological effects of structural modification of PTH and PTHrP at position 12 have been comprehensively evaluated with the finding that this position

tolerates a wide range of substitutions without substantial weakening of receptor interaction (41-43). Moreover, introduction of hydrophobic amino acids at position 12 enhances antagonist activity for PTH analogues without significantly affecting binding affinity for the PTHR1 (42); in addition to competitively antagonizing cAMP signaling at PTHR1 these substituted ligands can also act as inverse agonists that can reduces basal cAMP signaling at certain constitutively active PTHR1 variants (44).

The p.G43E variant segregated with isolated hypoparathyroidism in this family. The unaffected parents were heterozygous, while two affected sibs were also homozygous. One unaffected brother was heterozygous for the same nucleotide change and an unaffected sister was homozygous for the wild type nucleotide (Figure 1B). Serum levels of calcium were normal in the heterozygous subjects but levels of intact PTH were at the upper limits of normal or slightly increased, possibly due to co-existing vitamin D deficiency as serum phosphate levels were low or low normal (Table 1). The p.G43E variant is not present in either the Single Nucleotide Polymorphism Database or Exome Aggregation Consortium database, making unlikely the possibility that the variant is a rare polymorphism. Although *in silico* analyses classify p.G43E as a variant of unknown significance (VUS), when we ran a secondary structure prediction model on the wild type and p.G43E proteins using the Chou and Fasman Secondary Structure Prediction Server (CFSSP, http://www.biogem.org/tool/chou-fasman/) (Figure 4) we found that the amino acid replacement led to a critical disruption of the beta-strand (45). Taken together, the data indicate that this variant is likely to be pathogenic.

PTH Infusion

Subcutaneous administration of teriparatide to the proband (VI-2) and his affected brother (VI-3) from kindred B was performed when they were 8 and 10 years-of-age, respectively. This elicited normal (>10-fold) increases in urinary excretion of nephrogenous cAMP followed by corresponding normal (>20%) decreases in phosphate reabsorption (38, 39)(Figure 5A) and serum phosphate concentrations (Figure 4B) (46). In addition, the concentration of intact PTH-(1-84) in serum fell appropriately after injection of teriparatide, presumably in response to increasing serum concentrations of total calcium that also led to increases in urinary calcium excretion (Figure 5B) (46). These responses indicate that renal responsiveness to PTH was completely intact and was not antagonized by elevated circulating levels of bioinactive PTH (1-84).

Discussion

Genetic defects are uncommon causes of hypoparathyroidism but should be purposefully considered in young children with early-onset or congenital hypoparathyroidism (47). The two families that we describe in this report provide relevant lessons about PTH biochemistry as well as the evolving approach to contemporary molecular diagnosis. Levels of serum intact PTH were low in the proband of family A, which led clinicians to initially consider embryological defects in parathyroid development as the basis for hypoparathyroidism. By contrast, serum levels of intact PTH were markedly elevated in affected subjects in family B, which prompted studies to evaluate a possible form of autosomal recessive PHP type 1b (40) as the basis. In both cases initial studies were non-informative, and ultimately the correct diagnoses were established through gene-agnostic molecular testing that utilized next generation sequencing techniques. Thus, these cases argue for a diagnostic algorithm in which genetic testing occurs early during evaluation of hypoparathyroidism, and which

while perhaps less satisfying intellectually is ultimately more expedient (and cost-effective) functionally.

Mutations of the *PTH* gene are uncommon but they may be underrecognized cause of hypoparathyroidism due to genetic defects that lead to low or undetectable levels of immunoreactive PTH in the serum. The human *PTH* gene contains 3 exons; exon 1 is noncoding while exons 2 and 3 encode preproPTH (48-50) (Figure 2). The preproPTH messenger RNA (mRNA) encodes an amino-terminal 25-amino-acid leader or signal peptide that directs the nascent chain into the ER, where it is co-translationally cleaved by the signalase enzyme. The 6-amino-acid propeptide is subsequently removed by proprotein convertases, after trafficking to the Golgi apparatus, thereby yielding the mature 84-amino-acid PTH polypeptide. Defects in the PTH gene can cause hypoparathyroidism through several different mechanisms (16). For example, mutations can lead to abnormal splicing of preproPTH mRNA (17), disrupt processing of preproPTH protein (51-53), or generate bioinactive PTH molecules (22, 23).

In the proband of family A we identified a novel heterozygous missense mutation, p.A16K, in the hydrophobic core of the leader sequence that is flanked by two previously identified missense mutations, p.M14K (19) and p.C18R (18) that had been shown to cause autosomal dominant isolated hypoparathyroidism via inhibition of the normal processing of preproPTH to proPTH (19, 21). Functional assays in HEK293 cells demonstrated much greater intracellular retention of these mutant proteins, principally in the ER, with induction of ER stress and apoptosis that could be prevented by addition of the chemical chaperone 4-phenylbutyrate (4-PBA) to the cell culture medium (19, 20). These observations raise the possibility that 4-PBA, or another protein chaperone, might be useful as a rescue therapy (54) to restore PTH secretion and/or preserve parathyroid cell mass in patients with *PTH* gene mutations that impair function of the signal peptide.

In family B we identified a novel missense mutation, p.G43E, that replaces the highly conserved amino acid 12 in mature PTH with glutamic acid and results in a molecule that lacks PTH bioactivity *in vivo* but is recognized by second-generation immunoassays for intact PTH (Figure 2). Second-generation assays are sandwich immunoassays in which a capture antibody is directed against the C-terminal portion of mature PTH (residues 39 to 84) and a second detector antibody that is directed against epitopes within the N-terminal part of the molecule (13-34) (55). Although these assays were supposed to measure only full-length PTH, the later discovery of amino terminally truncated PTH fragments such as PTH (7-84) that can antagonize PTHR1 signaling led to the development of third-generation "whole molecule" PTH assays that utilized detector antibodies directed against amino acids 1-4 (56). Two previous examples of bioinactive PTH molecules have been reported. In one case, replacement of serine by proline (p.S32P) at the position of the first amino acid in mature PTH (1-84) did not interfere with detection by second-generation assays (23). By contrast, the other mutation, p.R56C, which led to replacement of arginine by cysteine in position 25 of mature PTH, generated a PTH molecule that showed reduced reactivity when measured with an intact PTH assay (22). The discordant results between p.R56C and p.G43E (position 12 in mature PTH) in assays for intact PTH likely results from epitopes used in assays for intact PTH. Today, most assays for intact PTH are immunometric assays that use two distinct antibodies, a capture antibody usually directed against a carboxyl-terminal portion of PTH(1-84) and detector antibodies that are directed against an antigenic site located around amino acids 20 to 25 of mature PTH (57). The assay that we used to measure intact PTH in members of this family was a sandwich assay in which a biotinylated monoclonal capture antibody reacts with epitopes in the N-terminal amino acid regions 26-32, which would predict full reactivity of this assay with the bioinactive PTH molecules with replacement of residue 12 in kindred B and less predictable behavior with the bioinactive p.R56C PTH containing a substitution at residue 25. Unfortunately, it was not possible to assess the immunoreactivity of PTH pG43E in other assays, including assays for whole molecule PTH.

The basis for the lack of bioactivity of p.G43E PTH is likely to be disruption of secondary structure. Gly43, which corresponds to amino acid 12 of mature PTH, is within the N-terminal region (residues 1–14) of the peptide that binds to the transmembrane helices and extracellular connecting loops (site 2) of PTHR1 and occupies the orthosteric pocket. Bimodal interaction of PTH with the PTHR1 is achieved through binding of a second sequence, residues 15–34, to an elongated hydrophobic groove on the extracellular domain of the receptor termed site 1 (58). Both of these binding regions form alpha helices that are connected by a beta-turn that provides a highly flexible mid-region (59). Despite the flexible nature of glycine, Gly12 is in a strict helical conformation in the crystal structure of PTH 1-34 (59). Substitution of Gly12 with alanine, a helix promotor, in [Tyr34]hPTH-(1–34)NH2 was well tolerated, whereas substitution with proline, a helix breaker, decreased receptor binding affinity 840-fold and adenylyl cyclase-stimulating activity 3500-fold (42). Our analyses indicated that replacement of Gly12 by Glu leads to a loss of the beta-sheet in the PTH molecule thereby disrupting the two distinct alpha-helices needed to achieve bimodal binding to the PTHR1. Together, these findings indicate that Gly12 is essential for full biological activity of PTH and that replacement by polar glutamate disrupts the required secondary structure needed for binding and activation of the PTHR1.

In conclusion, we report two new mutations in the *PTH* gene that cause familial isolated hypoparathyroidism through differing mechanisms. These mutations expand the number of pathogenic mutations in the *PTH* gene and emphasize the importance of considering the *PTH* gene as a cause of hypoparathyroidism in patients with either elevated or undetectable serum levels of immunoreactive PTH.

Data Availability Statement

Data sharing is not applicable to this article as no datasets were generated or analyzed during the current study.

References

1. **Thakker RV** 2004 Diseases associated with the extracellular calcium-sensing receptor. Cell Calcium. 35:275-282
2. **Nesbit MA, Hannan FM, Howles SA, Babinsky VN, Head RA, Cranston T, Rust N, Hobbs MR, Heath H, 3rd, Thakker RV** 2013 Mutations affecting G-protein subunit alpha11 in hypercalcemia and hypocalcemia. N Engl J Med 368:2476-2486
3. **Li D, Opas EE, Tuluc F, Metzger DL, Hou C, Hakonarson H, Levine MA** 2014 Autosomal dominant hypoparathyroidism caused by germline mutation in GNA11: phenotypic and molecular characterization. J Clin Endocrinol Metab 99:E1774-1783
4. **Mannstadt M, Harris M, Bravenboer B, Chitturi S, Dreijerink KM, Lambright DG, Lim ET, Daly MJ, Gabriel S, Juppner H** 2013 Germline mutations affecting Galpha11 in hypoparathyroidism. N Engl J Med 368:2532-2534
5. **Roszko KL, Bi RD, Mannstadt M** 2016 Autosomal Dominant Hypocalcemia (Hypoparathyroidism) Types 1 and 2. Frontiers in physiology 7:458
6. **Ding C, Buckingham B, Levine MA** 2001 Familial isolated hypoparathyroidism caused by a mutation in the gene for the transcription factor GCMB. J Clin Invest 108:1215-1220
7. **Yi HS, Eom YS, Park Ie B, Lee S, Hong S, Juppner H, Mannstadt M, Lee S** 2012 Identification and characterization of C106R, a novel mutation in the DNA-binding domain of GCMB, in a family with autosomal-dominant hypoparathyroidism. Clin Endocrinol (Oxf) 76:625-633
8. **Park SY, Eom YS, Choi B, Yi HS, Yu SH, Lee K, Jin HS, Chung YS, Jung TS, Lee S** 2013 Genetic and clinical characteristics of korean patients with isolated hypoparathyroidism: from the Korean hypopara registry study. Journal of Korean medical science 28:1489-1495
9. **Sticht H, Hashemolhosseini S** 2006 A common structural mechanism underlying GCMB mutations that cause hypoparathyroidism. Medical hypotheses 67:482-487
10. **Mannstadt M, Bertrand G, Muresan M, Weryha G, Leheup B, Pulusani SR, Grandchamp B, Juppner H, Silve C** 2008 Dominant-negative GCMB

mutations cause an autosomal dominant form of hypoparathyroidism. J Clin Endocrinol Metab 93:3568-3576

11. **Canaff L, Zhou X, Mosesova I, Cole DE, Hendy GN** 2009 Glial cells missing-2 (GCM2) transactivates the calcium-sensing receptor gene: effect of a dominant-negative GCM2 mutant associated with autosomal dominant hypoparathyroidism. Human mutation 30:85-92
12. **Mirczuk SM, Bowl MR, Nesbit MA, Cranston T, Fratter C, Allgrove J, Brain C, Thakker RV** 2010 A missense glial cells missing homolog B (GCMB) mutation, Asn502His, causes autosomal dominant hypoparathyroidism. J Clin Endocrinol Metab 95:3512-3516
13. **Kebebew E, Peng M, Wong MG, Ginzinger D, Duh QY, Clark OH** 2004 GCMB gene, a master regulator of parathyroid gland development, expression, and regulation in hyperparathyroidism. Surgery 136:1261-1266
14. **Liu Z, Yu S, Manley NR** 2007 Gcm2 is required for the differentiation and survival of parathyroid precursor cells in the parathyroid/thymus primordia. Developmental biology 305:333-346
15. **Tonoki H, Narahara K, Matsumoto T, Niikawa N** 1991 Regional mapping of the parathyroid hormone gene (PTH) by cytogenetic and molecular studies. Cytogenet Cell Genet 56:103-104
16. **Lee JH, Davaatseren M, Lee S** 2020 Rare PTH Gene Mutations Causing Parathyroid Disorders: A Review. Endocrinol Metab (Seoul) 35:64-70
17. **Parkinson DB, Thakker RV** 1992 A donor splice site mutation in the parathyroid hormone gene is associated with autosomal recessive hypoparathyroidism. Nat Genet 1:149-152
18. **Arnold A, Horst SA, Gardella TJ, Baba H, Levine MA, Kronenberg HM** 1990 Mutation of the signal peptide-encoding region of the preproparathyroid hormone gene in familial isolated hypoparathyroidism. J Clin Invest 86:1084-1087
19. **Cinque L, Sparaneo A, Penta L, Mencarelli A, Rogaia D, Esposito S, Fabrizio FP, Baorda F, Verrotti A, Falorni A, Stangoni G, Hendy GN, Guarnieri V, Prontera P** 2017 Autosomal Dominant PTH Gene Signal Sequence Mutation in a Family With Familial Isolated Hypoparathyroidism. J Clin Endocrinol Metab 102:3961-3969

20. **Datta R, Waheed A, Shah GN, Sly WS** 2007 Signal sequence mutation in autosomal dominant form of hypoparathyroidism induces apoptosis that is corrected by a chemical chaperone. Proc Natl Acad Sci U S A 104:19989-19994
21. **Karaplis AC, Lim SK, Baba H, Arnold A, Kronenberg HM** 1995 Inefficient membrane targeting, translocation, and proteolytic processing by signal peptidase of a mutant preproparathyroid hormone protein. J Biol Chem 270:1629-1635
22. **Lee S, Mannstadt M, Guo J, Kim SM, Yi HS, Khatri A, Dean T, Okazaki M, Gardella TJ, Juppner H** 2015 A Homozygous [Cys25]PTH(1-84) Mutation That Impairs PTH/PTHrP Receptor Activation Defines a Novel Form of Hypoparathyroidism. J Bone Miner Res 30:1803-1813
23. **Gild ML, Bullock M, Luxford C, Field M, Clifton-Bligh RJ** 2020 Congenital Hypoparathyroidism Associated With Elevated Circulating Nonfunctional Parathyroid Hormone Due to Novel PTH Mutation. J Clin Endocrinol Metab 105
24. **Li D, Bupp C, March ME, Hakonarson H, Levine MA** 2020 Intragenic Deletions of GNAS in Pseudohypoparathyroidism Type 1A Identify a New Region Affecting Methylation of Exon A/B. J Clin Endocrinol Metab 105
25. **Li H, Durbin R** 2009 Fast and accurate short read alignment with Burrows-Wheeler transform. Bioinformatics 25:1754-1760
26. **DePristo MA, Banks E, Poplin R, Garimella KV, Maguire JR, Hartl C, Philippakis AA, del Angel G, Rivas MA, Hanna M, McKenna A, Fennell TJ, Kernytsky AM, Sivachenko AY, Cibulskis K, Gabriel SB, Altshuler D, Daly MJ** 2011 A framework for variation discovery and genotyping using next-generation DNA sequencing data. Nat Genet 43:491-498
27. **Manichaikul A, Mychaleckyj JC, Rich SS, Daly K, Sale M, Chen WM** 2010 Robust relationship inference in genome-wide association studies. Bioinformatics 26:2867-2873
28. **Adzhubei IA, Schmidt S, Peshkin L, Ramensky VE, Gerasimova A, Bork P, Kondrashov AS, Sunyaev SR** 2010 A method and server for predicting damaging missense mutations. Nat Methods 7:248-249

29. **Sim NL, Kumar P, Hu J, Henikoff S, Schneider G, Ng PC** 2012 SIFT web server: predicting effects of amino acid substitutions on proteins. Nucleic Acids Res 40:W452-457
30. **Schwarz JM, Cooper DN, Schuelke M, Seelow D** 2014 MutationTaster2: mutation prediction for the deep-sequencing age. Nature methods 11:361-362
31. **Richards S, Aziz N, Bale S, Bick D, Das S, Gastier-Foster J, Grody WW, Hegde M, Lyon E, Spector E, Voelkerding K, Rehm HL, Committee ALQA** 2015 Standards and guidelines for the interpretation of sequence variants: a joint consensus recommendation of the American College of Medical Genetics and Genomics and the Association for Molecular Pathology. Genet Med 17:405-424
32. **Qian N, Sejnowski TJ** 1988 Predicting the secondary structure of globular proteins using neural network models. Journal of molecular biology 202:865-884
33. **Garnier J, Osguthorpe DJ, Robson B** 1978 Analysis of the accuracy and implications of simple methods for predicting the secondary structure of globular proteins. Journal of molecular biology 120:97-120
34. **Prevelige P, Fasman GD** 1989 Chou-Fasman prediction of the secondary structure of proteins. In: Prediction of protein structure and the principles of protein conformation: Springer; 391-416
35. **Almagro Armenteros JJ, Tsirigos KD, Sønderby CK, Petersen TN, Winther O, Brunak S, von Heijne G, Nielsen H** 2019 SignalP 5.0 improves signal peptide predictions using deep neural networks. Nat Biotechnol 37:420-423
36. **Danzig J, Li D, Jan de Beur S, Levine MA** 2021 High-Throughput Molecular Analysis of Pseudohypoparathyroidism 1b Patients Reveals Novel Genetic and Epigenetic Defects. J Clin Endocrinol Metab
37. **Walton RJ, Bijvoet OL** 1975 Nomogram for derivation of renal threshold phosphate concentration. Lancet 2:309-310
38. **Mallette LE, Kirkland JL, Gagel RF, Law WM, Jr., Heath H, 3rd** 1988 Synthetic human parathyroid hormone-(1-34) for the study of pseudohypoparathyroidism. J Clin Endocrinol Metab 67:964-972
39. **Mallette LE** 1988 Synthetic human parathyroid hormone 1-34 fragment for diagnostic testing. Annals of internal medicine 109:800-804

40. **Fernández-Rebollo E, Pérez de Nanclares G, Lecumberri B, Turan S, Anda E, Pérez-Nanclares G, Feig D, Nik-Zainal S, Bastepe M, Jüppner H** 2011 Exclusion of the GNAS locus in PHP-Ib patients with broad GNAS methylation changes: evidence for an autosomal recessive form of PHP-Ib? J Bone Miner Res 26:1854-1863
41. **Goldman ME, McKee RL, Caulfield MP, Reagan JE, Levy JJ, Gay CT, DeHaven PA, Rosenblatt M, Chorev M** 1988 A new highly potent parathyroid hormone antagonist: [D-Trp12,Tyr34]bPTH-(7-34)NH2. Endocrinology 123:2597-2599
42. **Chorev M, Goldman ME, McKee RL, Roubini E, Levy JJ, Gay CT, Reagan JE, Fisher JE, Caporale LH, Golub EE, et al.** 1990 Modifications of position 12 in parathyroid hormone and parathyroid hormone related protein: toward the design of highly potent antagonists. Biochemistry 29:1580-1586
43. **Peggion E, Mammi S, Schievano E, Silvestri L, Schiebler L, Bisello A, Rosenblatt M, Chorev M** 2002 Structure-function studies of analogues of parathyroid hormone (PTH)-1-34 containing beta-amino acid residues in positions 11-13. Biochemistry 41:8162-8175
44. **Cheloha RW, Gellman SH, Vilardaga J-P, Gardella TJ** 2015 PTH receptor-1 signalling—mechanistic insights and therapeutic prospects. Nature Reviews Endocrinology 11:712-724
45. **Kumar TA** 2013 CFSSP: Chou and Fasman secondary structure prediction server. Wide Spectrum 1:15-19
46. **Lindsay R, Nieves J, Henneman E, Shen V, Cosman F** 1993 Subcutaneous administration of the amino-terminal fragment of human parathyroid hormone-(1-34): kinetics and biochemical response in estrogenized osteoporotic patients. J Clin Endocrinol Metab 77:1535-1539
47. **Gordon RJ, Levine MA** 2018 Genetic Disorders of Parathyroid Development and Function. Endocrinol Metab Clin North Am 47:809-823
48. **Goswami R, Mohapatra T, Gupta N, Rani R, Tomar N, Dikshit A, Sharma RK** 2004 Parathyroid hormone gene polymorphism and sporadic idiopathic hypoparathyroidism. J Clin Endocrinol Metab 89:4840-4845
49. **Vasicek TJ, McDevitt BE, Freeman MW, Fennick BJ, Hendy GN, Potts JT, Jr., Rich A, Kronenberg HM** 1983 Nucleotide sequence of the human parathyroid hormone gene. Proc Natl Acad Sci U S A 80:2127-2131

50. **Reis A, Hecht W, Groger R, Bohm I, Cooper DN, Lindenmaier W, Mayer H, Schmidtke J** 1990 Cloning and sequence analysis of the human parathyroid hormone gene region. Hum Genet 84:119-124
51. **Ertl DA, Stary S, Streubel B, Raimann A, Haeusler G** 2012 A novel homozygous mutation in the parathyroid hormone gene (PTH) in a girl with isolated hypoparathyroidism. Bone 51:629-632
52. **Sunthornthepvarakul T, Churesigaew S, Ngowngarmratana S** 1999 A novel mutation of the signal peptide of the preproparathyroid hormone gene associated with autosomal recessive familial isolated hypoparathyroidism. J Clin Endocrinol Metab 84:3792-3796
53. **Baran N, ter Braak M, Saffrich R, Woelfle J, Schmitz U** 2015 Novel activating mutation of human calcium-sensing receptor in a family with autosomal dominant hypocalcaemia. Mol Cell Endocrinol 407:18-25
54. **Singh OV, Pollard HB, Zeitlin PL** 2008 Chemical rescue of deltaF508-CFTR mimics genetic repair in cystic fibrosis bronchial epithelial cells. Mol Cell Proteomics 7:1099-1110
55. **Couchman L, Taylor DR, Krastins B, Lopez MF, Moniz CF** 2014 LC-MS candidate reference methods for the harmonisation of parathyroid hormone (PTH) measurement: a review of recent developments and future considerations. Clin Chem Lab Med 52:1251-1263
56. **Lepage R, Roy L, Brossard JH, Rousseau L, Dorais C, Lazure C, D'Amour P** 1998 A non-(1-84) circulating parathyroid hormone (PTH) fragment interferes significantly with intact PTH commercial assay measurements in uremic samples. Clin Chem 44:805-809
57. **Vieira JG** 2012 PTH Assays: Understanding What We Have and Forecasting What We Will Have. J Osteoporos 2012:523246
58. **Ehrenmann J, Schöppe J, Klenk C, Rappas M, Kummer L, Doré AS, Plückthun A** 2018 High-resolution crystal structure of parathyroid hormone 1 receptor in complex with a peptide agonist. Nat Struct Mol Biol 25:1086-1092
59. **Jin L, Briggs SL, Chandrasekhar S, Chirgadze NY, Clawson DK, Schevitz RW, Smiley DL, Tashjian AH, Zhang F** 2000 Crystal structure of human parathyroid hormone 1-34 at 0.9-A resolution. J Biol Chem 275:27238-27244

Figure Legends

Figure 1: Pedigrees of the two investigated families. Subjects with biochemical hypoparathyroidism are depicted by solid-colored symbols while unaffected subjects are depicted by open symbols. Those subjects who underwent genetic testing have genotypes below the symbol; WT is a wild type *PTH* gene allele and M is a mutant allele. Squares denote males and circles denote females. A. The proband, denoted by the arrow, is heterozygous for the *PTH* gene mutation and her parents are homozygous for wild type *PTH* alleles. B. The proband, denoted by the arrow, and two siblings are homozygous for the *PTH* gene mutation, while his parents and one brother are heterozygous.

Figure 2: Schematic representation of the PTH protein. The complete preproPTH molecule is shown in the center with positions of point mutations that affect the protein shown beneath the figure; positions of the three mutations that cause bioinactive PTH are also depicted above the figure in the mature, PTH 1-84 molecule. The lower figure shows preproPTH, which consists of 115 amino acids; the specific regions comprise a 25-amino acid pre sequence (-31 to -7), a 6-amino acid pro sequence (-6 to -1), and 84-amino acid mature PTH molecule (+1 to 84). The upper figure shows epitopes used for detection of whole PTH (1-4) or intact PTH (13-34) as well as the epitope used to capture PTH fragments (39-84) in conventional sandwich assays.

Figure 3: Evaluation of the preproPTH as a signal peptide using the SignalP hidden Markov model program. Panels: A shows wild type PTH 1-84; B shows p.A16K; C shows p.M14K; and D shows p.C18R proteins; black arrows denote replaced amino acids. A highly relevant probability score was obtained for likelihood of N-terminal signal sequence (dotted red line) and

likelihood is predicted for cleavage site (dotted green line). The wild type protein (A) has a strongly predicted signal peptide cleavage site between amino acids 25 and 26. Residues are numbered conventionally, with the first residue (M) of the preproPTH polypeptide designated as +1. See text for Methods.

Figure 4. Secondary structure predicted by the Chou-Fasman algorithm. We used the CFSPP online server to analyze the predicted locations of alpha-helix and beta-strand from the amino acid sequence of wild type (A) and p.G43E (B) PTH proteins. In each panel, a black arrow denotes either the wild type amino acid or the substituted amino acid at position 43. Alpha helices are shown in red and beta strands are shown in blue.

Figure 5. Teriparatide infusion in two affected subjects from family B. Effects of teriparatide on affected subjects VI-2 (left) and VI-3 (right) are shown. Teriparatide (40 μg) was administered subcutaneously at time 0. Upper panels (A) show the changes in urinary excretion of cAMP and TmP/GFR after infusion; lower panels (B) show changes in serum levels of calcium, phosphate and intact PTH as well as urinary ca:cr ratio.

Table 1. Clinical and Biochemical Characteristics of Members of Family B

Family member	Clinical status	Current Age, yrs	Sex	PTH genotype	sCa, mmol/L	sPhos, mmol/L	iCa, mmol/L	25(OH)D, nmol/L	1,25(OH)$_2$D, pmol/L	intact PTH, pmol/L
Reference range					2.15-2.55	1.05-1.8	1.1-1.3	50-150	48-192	1.6-6.9
V-8	Affected	40	F	ND*	1.8	1.46	0.91	36.5		9.3
V-9	Affected	25	F	ND	1.65	2.06		36.2		19.1
V-11	Unaffected	32	F	Het	2.39	0.82	1.22	33.7		6.4
V-12	Unaffected	35	M	Het	2.32	0.95	1.28	23.8		8.1
V-22	Affected	36	F	ND	1.76	1.52		66.2		32.2
VI-1	Unaffected	12	M	HET	2.35	1.11		29		6.8
VI-2	Affected	11	M	HOM	1.7	2.61	0.89	14	29	23.8
VI-3	Affected	9	M	HOM	1.69	2.28	0.85	56	<12	74
VI-4	Unaffected	5	F	WT	2.5	2.03				2.7
VI-5	Affected	2	F	HOM	1.7	3.16	0.97	84.7		76.9

*ND, not done.

Table 2. Methylation Analysis of *GNAS* DMRs in Family B

	NESP55 DMR methylation (%)	**XL DMR methylation (%)**	**A/B DMR methylation (%)**
Controls			
	45.9	38.2	50.1
	39.4	34.7	49.2
	41.2	39.1	51.9
Mean ± SD	42.1 ± 3.4	37.3 ± 2.3	50.4 ± 1.4
Subjects			
VI-2	42.3	39.6	51.6
VI-3	40.8	45.7	51.8
Mean ± SD	41.5 ± 1.1	42.7 ± 4.3	51.7 ± 0.1

Figure 1

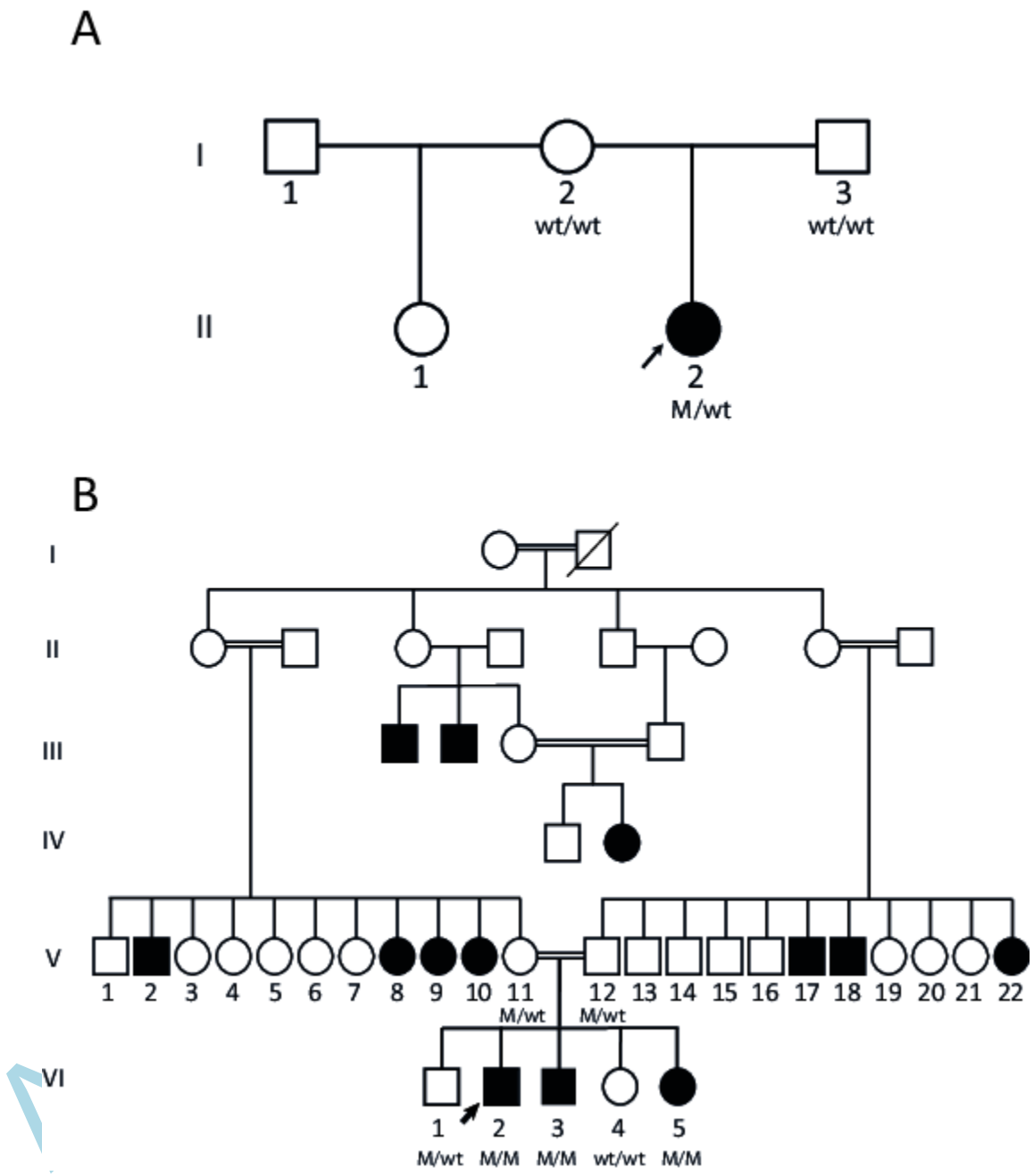

Figure 2

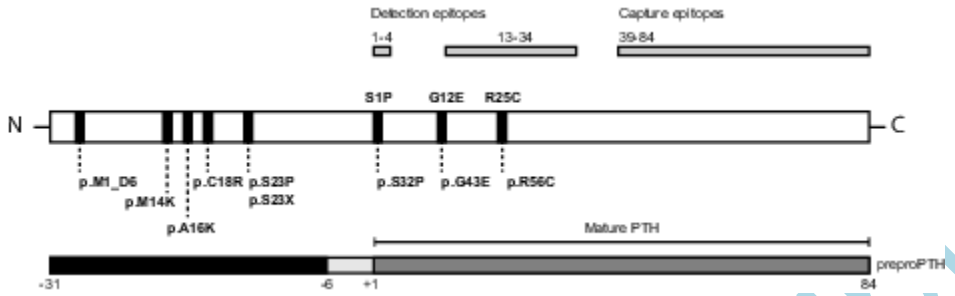

Figure 3

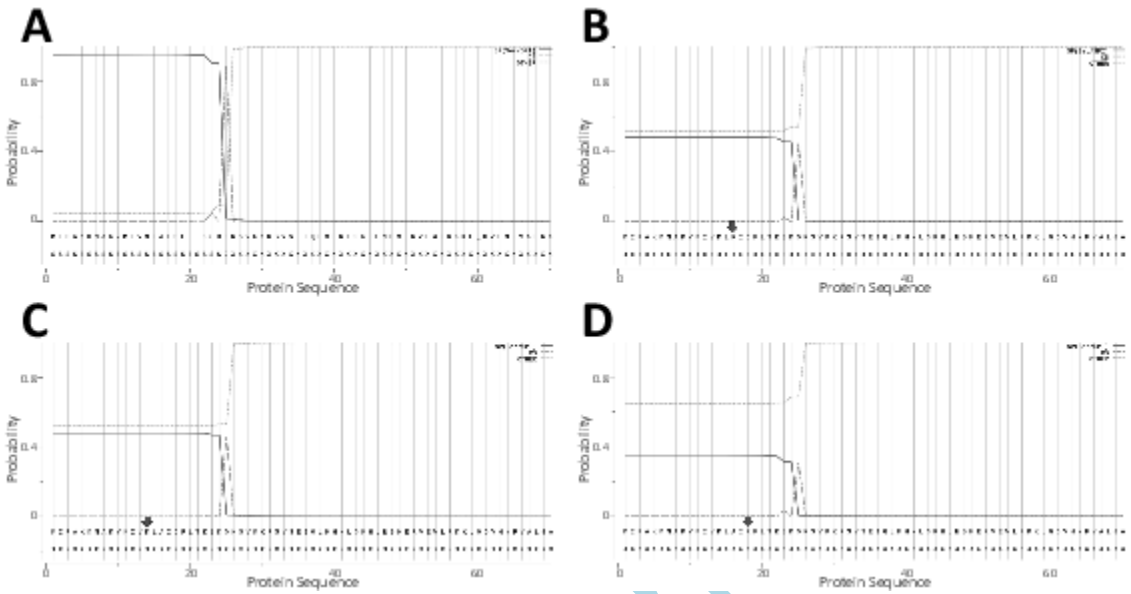

Figure 4

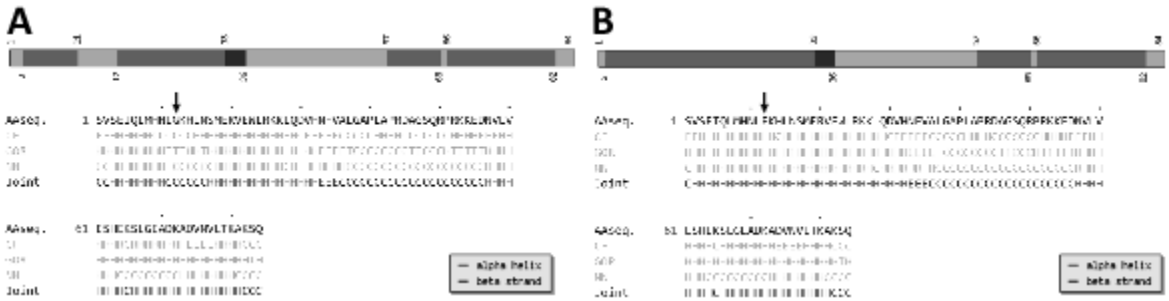

Figure 5